



# Projected Effects of Climate-induced Changes in Phytoplankton Biomass in the Southern South China Sea

Chathumini W. Kiel<sup>1,4</sup>, Kanchana Bandara<sup>2</sup>, Roswati MD Amin<sup>3</sup>, Nathalie Gypens<sup>4</sup>, Mohd Fadzil Mohd Akhir<sup>1</sup>

- <sup>1</sup>Institute of Oceanography and Environment, Universiti Malaysia Terengganu, Kuala Nerus, 21030, Malaysia
  - <sup>2</sup>Akvaplan-niva, Fram Centre, Tromsø, 9296, Norway
  - <sup>3</sup>Faculty of Science and Marine Environment, Universiti Malaysia Terengganu, Kuala Nerus, 21030, Malaysia
  - <sup>4</sup>Laboratoire d'Ecologie des Systèmes Aquatiques, Université Libre de Bruxelles, Bruxelles, 1050, Belgium
- 10 Correspondence to: Mohd Fadzil Mohd Akhir (mfadzil@umt.edu.my)

Abstract. Phytoplankton lies at the base of the marine pelagic food webs influencing the planet's net primary production and nutrient cycles. Understanding the impacts of anthropogenic climate change on the phytoplankton dynamics is crucial due to their pivotal role. Numerous studies across various latitudes have investigated the effects of climate change on the world's oceans, focusing on future projections on plankton. However, despite being one of the largest marginal seas of the world, the impact of such future projections on marine plankton in the South China Sea has rarely been documented. Monsoon derived productive upwelling areas in the South China Sea serve as ideal sites for studying plankton dynamics. In this study, a 3D coupled physical-biogeochemical model is used to examine the response of phytoplankton biomass and selected abiotic and biotic factors to future anthropogenic climate change, focusing on two upwelling areas of the southern South China Sea: southeast Vietnam and northwest Sabah. The results show declined phytoplankton biomass associated with warming and nutrient depletion, particularly silicate. However, the grazing pressure by mesozooplankton is predicted to be reduced, suggesting that this studied system is under bottom-up control. This study highlights the anticipated amplification of climate change-induced impacts on the phytoplankton over to higher trophic levels, which may influence both ecosystems and socioeconomics in the region.

# 1 Introduction

25 Phytoplankton plays a crucial role in Earth's ecosystems, representing only 1% of planet's photosynthetic biomass, yet contributing to nearly half of the global net primary production (Field et al., 1998). Beyond their primary production role, phytoplankton contributes significantly to nutrient recycling while actively shaping marine food webs (Behrenfeld et al., 2006; Naselli-Flores & Padisák, 2023). Phytoplankton are microscopic organisms that are highly responsive to short and long-term environmental changes, exerting considerable influence on the dynamics of marine ecosystems. Their impact extends further into critical processes, including biogeochemical cycles and the structure of marine food webs (Yuan et al., 2018).



65



Since the onset of the industrial era, a substantial quantity of greenhouse gases has been discharged into the atmosphere due to human activities, causing noteworthy environmental changes (Pagès et al., 2020). According to the records, the average atmospheric carbon dioxide (CO<sub>2</sub>) concentration, that remained around 280 ppm in the pre-industrial era, reached 419 ppm in 2023(Lindsey, 2024). About 1/3 of these anthropogenically emitted atmospheric CO<sub>2</sub> is absorbed by the ocean, and therefore it plays a crucial role among the processes contributing to the removal of CO<sub>2</sub> from the atmosphere (Cao et al., 2009). However, as more CO<sub>2</sub> is being emitted, the increased ocean uptake leads to several adverse effects on the ocean, including warming, acidification, and deoxygenation (Bindoff et al., 2019). The significance of plankton and their vulnerability to the ongoing effects of climate change underlines the necessity of exploring the long-term patterns of plankton in the global oceans (Hays et al., 2005). Previous studies have shown projected declines in global phytoplankton biomass in a changing climate, with much-pronounced declines expected in tropical and subtropical regions (e.g., Bopp et al., 2013; Boyce et al., 2010; Henson et al.; 2021; Marinov et al., 2010). However, variations in regional climate patterns may introduce fluctuations around these projected trends (Boyce et al., 2010), highlighting the importance of carrying out climate studies on regional scales.

The South China Sea (SCS), which is among the world's largest marginal seas, has its unique variability due to the influence of both seasonal monsoons and the adjacent oceanic currents (Hou et al., 2022). In addition to its unique climatic features, the SCS retains its significance due to its vital role in fisheries, contributing to its socio-economic value (Pauly & Liang, 2020). Despite its importance, the studies on the impact of climate change on future plankton biomass in the SCS is less focused. Contrary to other marginal seas in the world such as the Mediterranean Sea (Pagès et al., 2020) and the Bering Sea (Chen et al., 2021; Hermann et al., 2013), studies have rarely used a modelling approach to form a future projection of the plankton dynamics in the SCS under climate change scenarios. Understanding these specific future impacts of climate change on the lower trophic levels helps to reflect its potential pressures on biodiversity as well as commercial fishing and socioeconomics in this region. This knowledge aids in developing mitigation strategies and the adaptation of appropriate policy frameworks.

This research primarily focuses on studying potential temporal and spatial shifts in the phytoplankton biomass, along with the key abiotic and biotic factors influencing these changes, in two selected upwelling areas of the southern SCS driven by projected climate change impacts. Specifically, this study has focused on ocean warming from 1990 until year 2060, as outlined in the IPCC RCP8.5(IPCC, 2014) emission scenario. In this study, the key external environmental factors chosen for analysis include temperature, nitrate and silicate as abiotic attributes (bottom-up drivers), and grazer/predator biomass as a biotic attribute (top-down driver) all of which are known to have major influence on phytoplankton biomass (Winder & Sommer, 2012). Since upwelling areas are extensively used as focal areas of phytoplankton research due to their role of bringing nutrient rich sub-surface waters to the sea surface and significantly enhancing phytoplankton blooms (Wu et al., 2019), the present study focuses on two key upwelling areas in the southern SCS. These are, the southeast Vietnam upwelling area and the northwest Sabah upwelling area, both of which experience upwelling activity during monsoon seasons. Using model outputs from a specifically designed regional coupled 3-dimensional biophysical model, this research

https://doi.org/10.5194/egusphere-2025-4988 Preprint. Discussion started: 17 November 2025

© Author(s) 2025. CC BY 4.0 License.





aims to assess temporal and spatial dynamics of the phytoplankton biomass and the selected abiotic and biotic environmental factors in the above upwelling areas during their respective monsoon seasons. Furthermore, the probable underlying relationships between the model-predicted spatio-temporal phytoplankton trends and external factors are discussed both in bottom-up and top-down regulatory contexts.

#### 2 Materials and Methods

## 2.1 Study Area

75

The South China Sea (SCS) is a tropical, semi-enclosed shallow continental shelf in the Western Pacific Ocean, bordered by the land masses of east and west Malaysia, Vietnam, and Indonesia (Akhir, 2012). This region experiences distinct seasonal monsoons, where it is subjected to north-eastern monsoon (winter) and south-western monsoon (summer) from November to March and April to August, respectively. This area's bathymetry is characterized by shallow waters (< 100 m) over the shelf area which extends to deeper offshores (> 300 m) (Apriansyah et al., 2022). The surface circulation of SCS undergoes significant seasonal variations, influenced by these alternating monsoons, which could potentially change its biogeochemistry (Liu et al., 2002). These monsoonal winds induce coastal upwelling, giving rise to seasonally productive waters such as in the southern Vietnam (Zhao et al., 2018), eastern coast of peninsular Malaysia (Akhir et al., 2015) and northwestern Sabah region on Borneo Island (Satar et al., 2020). However, this study focusses only on two upwelling regions: southeastern Vietnam extending from 109–113°E and 9–13 °N (Wu et al., 2019) and northwestern Sabah extending from 114.5–118°E and 4.5–8 °N (Satar et al., 2020) (Figure 1). Upwelling occurs in the southeast Vietnam region during the summer, while in northwest Sabah, it takes place during the winter monsoon season. Moreover, to analyse the vertical profiles within these areas, coordinates were used based on previous studies in the southeast Vietnam upwelling region (Xiao et al., 2020) and the northwest Sabah upwelling region (Satar et al., 2020).





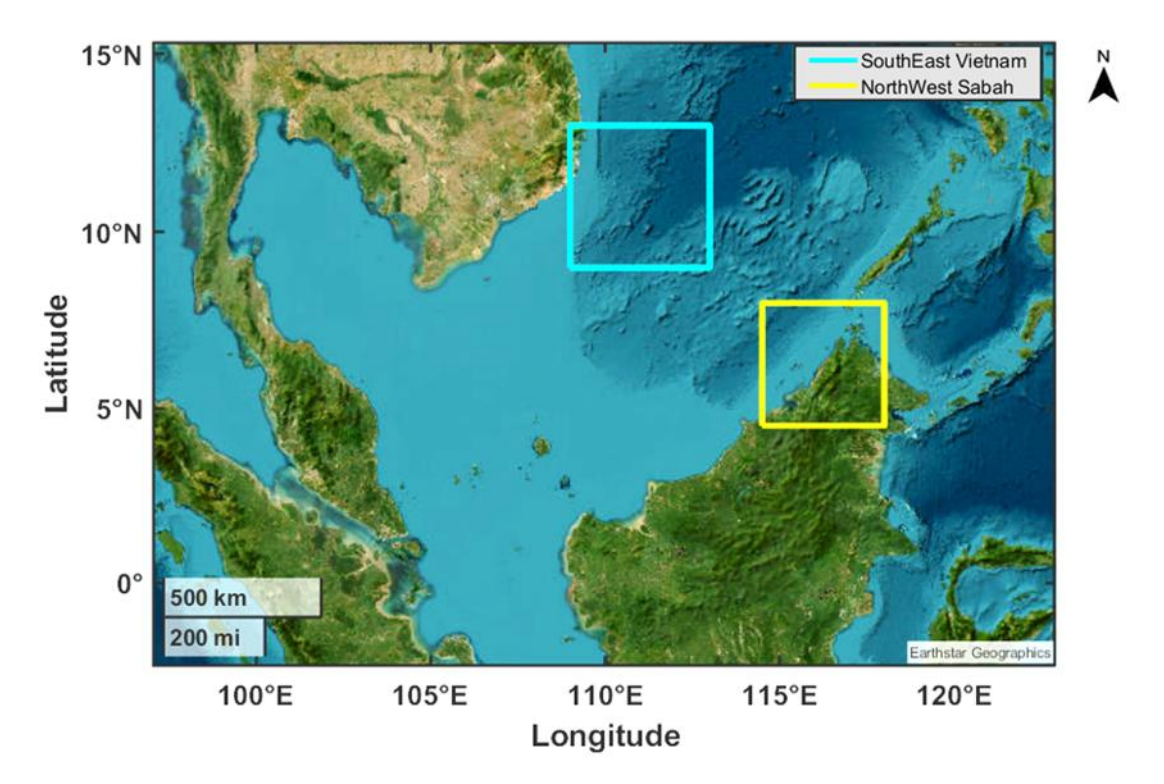


Figure 1:Map of the study area. The blue bounding box with coordinate ranges 109–113°E and 9–13 °N shows the southeast Vietnam upwelling region and yellow bounding box with coordinate ranges 114.5–118°E and 4.5–8 °N shows the northwest Sabah upwelling region.

## 00 2.2 The data sets

95

100

To study the dynamics of phytoplankton biomass in the SSCS upwelling regions in response to potential anthropogenic climate change, a pre-defined spatiotemporal subset from the validated simulation outputs of the SEAsia model (South East Asia Model) (see Section 2.2.1 below) was used as the main input dataset. In addition, to compare the SEAsia model outputs for selected variables with contemporary observations, satellite-derived datasets from Copernicus marine services were used as supporting datasets. These were: (i) Global Ocean OSTIA Sea Surface Temperature and Sea Ice Analysis (<a href="https://doi.org/10.48670/moi-00165">https://doi.org/10.48670/moi-00165</a>) and (ii) Global Ocean Colour (Copernicus-GlobColour), Bio-Geo-Chemical, L3 (daily) from Satellite Observations (Near Real Time) (<a href="https://doi.org/10.48670/moi-00278">https://doi.org/10.48670/moi-00278</a>).

## 2.2.1 Overview of the SEAsia model

The Southeast Asia (SEAsia: https://github.com/NOC-MSM/SEAsia) model is a 3-dimensional (3D) regional configuration of the Nucleus for European Modelling of the Ocean (NEMO) coupled with a 1D biogeochemical model (see below). This coupled 3D model features a 1/12-degree (9 km) resolution with 75 vertical levels incorporating hybrid-z coordinates and it uses the ORCA12 bathymetry (DRAKKAR Group, 2007).



105

110

115

120

125



The atmospheric conditions, including wind, short- and long-wave radiation, humidity, temperature, precipitation and pressure imposed on the model were derived from the HadGEM2 (CMIP5) Earth system model under the "historical climate" (1980-2004) and the "business as usual" IPCC RCP8.5 emission scenario (2005-2060). In addition, atmospheric CO2 levels are imposed on the biogeochemical model (historical climate + RCP8.5). The model's lateral boundary conditions and initial conditions are derived from the global ¼° NEMO-MEDUSA ROAM simulation using identical surface forcing. The model incorporates 34 tidal constituents (FES2014 tide model), applied both as tidal potential and as sea surface height and barotropic currents along the open lateral boundaries of the model.

The biogeochemical model coupled to the above SEAsia ocean circulation component is a comprehensive ecosystem model, named European Regional Seas Ecosystem Model (ERSEM: (Butenschön et al., 2016)). However, the ERSEM configuration coupled to the SEAsia model was slightly modified compared to the original ERSEM configuration, where Iron (Fe) cycle and Chlorophyll-a are not included in the SEAsia regional configuration. This model includes both pelagic and benthic ecosystem components whereas the present study focuses solely only on its pelagic part. The functional types of this ecosystem model are based on their ecosystem roles rather than specific species or taxa. The organisms in the ERSEM configuration are categorized into: (i) primary producers – i.e., picophytoplankton(<2μm), diatoms, nanophytoplankton (2-20μm), and microphytoplankton (>20μm), (ii) primary consumers – i.e., mesozooplankton, microzooplankton, and nanoflagellates; (iii) and bacterial decomposers, along with (iv) particulate and dissolved organic matter (POM, DOM) in the pelagic zone. The state variables of this model include major chemical components for each functional type (carbon, nitrogen, phosphorus, silicate) where, a set of modules compute the rates of change of its state variables, considering the environmental conditions of the surrounding water body, physiological processes and predator-prey interactions (Butenschön et al., 2016; https://github.com/NOC-MSM/SEAsia). This biogeochemical model employs fully dynamic stoichiometry for most of its functional types. The model dynamics of a living functional type are based on a standard organism influenced by the assimilation of carbon and nutrients into organic compounds through uptake. This also includes generic loss processes such as respiration, excretion, release, predation, and non-predatory (non-consumptive) mortality. A schematic diagram of the trophic interactions in the pelagic zone is shown in Figure 2.



135

140

145



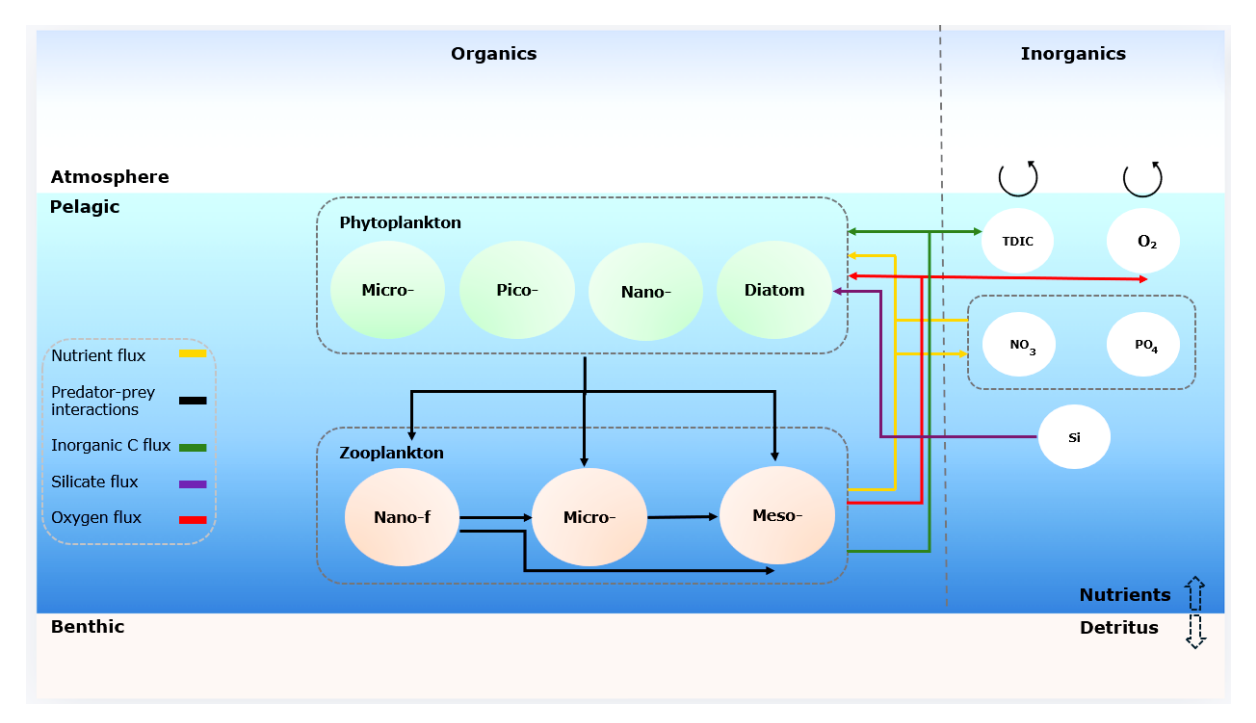


Figure 2:Schematic representation of the basic plankton interactions of the European Regional Seas Ecosystem Model (ERSEM).

## 2.2.2 Setting spatial, temporal and biological & environmental scopes

The spatial scope for the present study were the southeast Vietnam and northwest Sabha upwelling regions as described in Section 2.1 and Figure 1 at approximately 9 km resolution. On the vertical dimension, the scope was narrowed down to the upper 120 m of the water column, where much of the primary production occurs in the photic zone of this region (Zhu et al., 2021). Furthermore, an examination of vertical profiles shows that the peaks of all variables occurred consistently within this depth range (see: Supplementary). The temporal scope was a simulated timeseries extending from the year 1990 to 2060 (RCP8.5) at a monthly resolution. In terms of biology, the analyses focused mainly on the spatial and temporal dynamics of carbon biomass of phytoplankton. For the ease of analyses and interpretation, phytoplankton were divided into two classes: (i) diatom and (ii) non-diatom. The non-diatom biomass was considered as a unified (pooled) entity which is the sum of the carbon biomasses of picophytoplankton, nanophytoplankton and microphytoplankton. In this model, diatom group is characterized by their requirement of silicate, a characteristic not shared by other phytoplankton groups (Butenschön et al., 2016). For assessing the environmental dynamics, key variables (drivers) that are known to directly influence phytoplankton biomass were selected. These include seawater temperature and nutrient concentration - i.e., dissolved nitrate and silicate were selected as physicochemical (bottom-up) drivers. The grazer (mesozooplankton) biomass was selected as a biological driver that reflects the predation/grazing pressure on phytoplankton (top-down). The selected environmental variables, according to the model formulation and the previous studies, had the most significant forcing on phytoplankton entities of the SEAsia model (Butenschön et al., 2016; Winder & Sommer, 2012).



150

155

160

165

170

175



# 2.2.3 Comparing the model simulations and observations

As the first step, a comparison was made between the observed (satellite-derived) and model-simulated, mean sea surface temperature (SST) and phytoplankton carbon biomass during the upwelling monsoon seasons of a recent year (2023: present context) in southeast Vietnam and northwest Sabah upwelling areas. This comparison had to be made focusing on the surface layer (> 0.5 m) because satellite-derived data were based on the sea surface. Further, despite satellite-derived primary production estimates were in Chlorophyll-a units (Chl.-a), the SEAsia biogeochemical model did not include Chl.-a component in its outputs. Therefore, the satellite-derived Chl.-a concentrations were converted to carbon units (biomass carbon) using the Chl.-a: C ratio of 67.77(Xu et al., 2021).

### 2.2.4 Exploring temporal and spatial dynamics

As the first step of assessing the spatio-temporal patterns in the data, latitude-, longitude-, time- and depth-specific physicochemical (temperature, nutrients) and biological (diatom, non-diatom, mesozooplankton) data were extracted from the NetCDF4 files for the two upwelling regions separately. Here, the selected depth span (0-120 m) included 26 depth layers, where their arithmetic mean was obtained to reduce the spatial dimensionality of the data. Then, to further reduce temporal dimensionality of the data, these key variables were averaged over specific seasons, to allow for a more detailed analysis. In both upwelling regions, the productive season (= upwelling season) was focused on in the analyses. Here, in southeast Vietnam upwelling area, the analysis focused on the southwest or summer monsoon season (the average of months June, July and August) while in northwest Sabah upwelling area, it is on the northeast or winter monsoon season (the average of months December, January and February). When considering the temporal resolution, data on all the selected variables, except temperature, were calculated in monthly resolution. Due to this spatio-temporal dimensionality reduction, the southeast Vietnam data included vertically averaged information for the summer monsoon season, while northwest Sabah includes vertically averaged information for the winter monsoon season.

The dimensionality-reduced data were then used to study the: (i) temporal and (ii) spatial dynamics of phytoplankton (diatom and non-diatom) biomass, along with the selected key abiotic and biotic environmental variables that could potentially have driven these patterns. To study the temporal dynamics, timeseries analysis were performed on all variables across the two upwelling regions. For this, mean values for each variable were calculated separately for both the southeast Vietnam and northwest Sabah upwelling areas. Then, linear regression models were fitted to describe the overall trends or temporal patterns in the data. The adjusted R<sup>2</sup> values and the associated p-values of the fitted linear models were calculated on the observed trends of these timeseries to determine their significance. The observed trends were considered statistically significant at the 95% confidence level (= 0.05 significance level). In addition, seasonal anomalies were calculated and plotted to examine the interannual variability of the selected variables (The formula is given below where, N= 71(1990-2060) and i = year).



185

195

200



180 Seasonal anomaly = Seasonal mean<sub>i</sub> 
$$-\frac{1}{N}\sum_{j=1}^{N} seasonal mean_{j}$$
 (1)

Beside the observable temporal trends in the dataset, notable spatial variability existed (see Results). To study these spatial dynamics along the simulated timeseries, a two-step process was followed. Here, firstly, the timeseries was split into two sections, one focusing the proximal decade (1990-2000) and another focusing the distal decade (2050-2060) where the differential temporal change would be most pronounced under the simulated RCP8.5 based environmental forcing. Secondly, the percentage change of the phytoplankton (diatom and non-diatom) biomasses along with the other abiotic and biotic environmental variables across the two selected decades were calculated as:

$$Percentage\ change(\%) = \frac{(\mu_{2050-2060} - \mu_{1990-2000})}{\mu_{1990-2000}} * 100$$
 (2)

To further understand the environmental drivers underpinning the above temporal and spatial patterns in the data a principal component analysis (PCA) was performed for the two upwelling regions separately.

## 190 2.3 Software and packages used

Data pre-processing was conducted using R studio version 2023.12.1 build 402 (RStudio Team, 2023) with the 'ncdf4' package version 1.22 (Pierce, 2023). This step involved extracting specific coordinates of the selected domains, averaging the monthly values to obtain seasonal means, and averaging across depth layers. PCA plots were generated using the 'ggplot2' package version 3.5.1 (Wickham, 2016). All the remaining statistical tests and figures including the map of the study area were generated using The Math Works, Inc. (2023) MATLAB (Version 2023b).

#### 3 Results

#### 3.1 Model Skill Assessment

Figure 3 shows a comparison between modelled and the observed (satellite-derived) mean sea surface temperature (SST) and phytoplankton carbon biomass during the upwelling monsoon seasons of a recent year (2023: present context) in southeast Vietnam and northwest Sabah. In the southeast Vietnam upwelling region, both observed, and model-simulated temperature (Figure 3.a, e) indicate colder water masses near the coast, likely due to the upwelling of colder deeper waters during the summer monsoon season. The model-simulated mean SST (28.86°C over the entire southeast Vietnam domain) is not so different compared to the observed mean SST (29.10°C). In contrast, simulated SST in northwest Sabah upwelling region is notably higher compared to the observed data (mean = 29.72°C vs. 28.60°C: Figure 3.b, f). However, both observed and





simulated SST reveal a pattern of higher temperatures closer to the coast in the 115-116°E longitude range and lower temperatures near the coast in the southwestern sector of northwest Sabah (116-117°E longitude range).

With respect to carbon biomass, the modelled mean carbon biomass in southeast Vietnam (15.0 mgCm<sup>-3</sup> across the entire domain: Figure 3.g) is mostly similar to the observed entity (13.1 mgCm<sup>-3</sup>: Figure 3.c). However, in the northwest Sabah upwelling region, the modelled mean carbon biomass (11.1 mgCm<sup>-3</sup> over the entire domain: Figure 3.h) is approximately five times less than the observed mean carbon biomass (53.5 mgCm<sup>-3</sup>: Figure 3.d). In general, both across observed and simulated scenarios, the carbon biomass is closely associated with the temperature minimum closer to the coast, indicating strong upwelling-driven primary production.

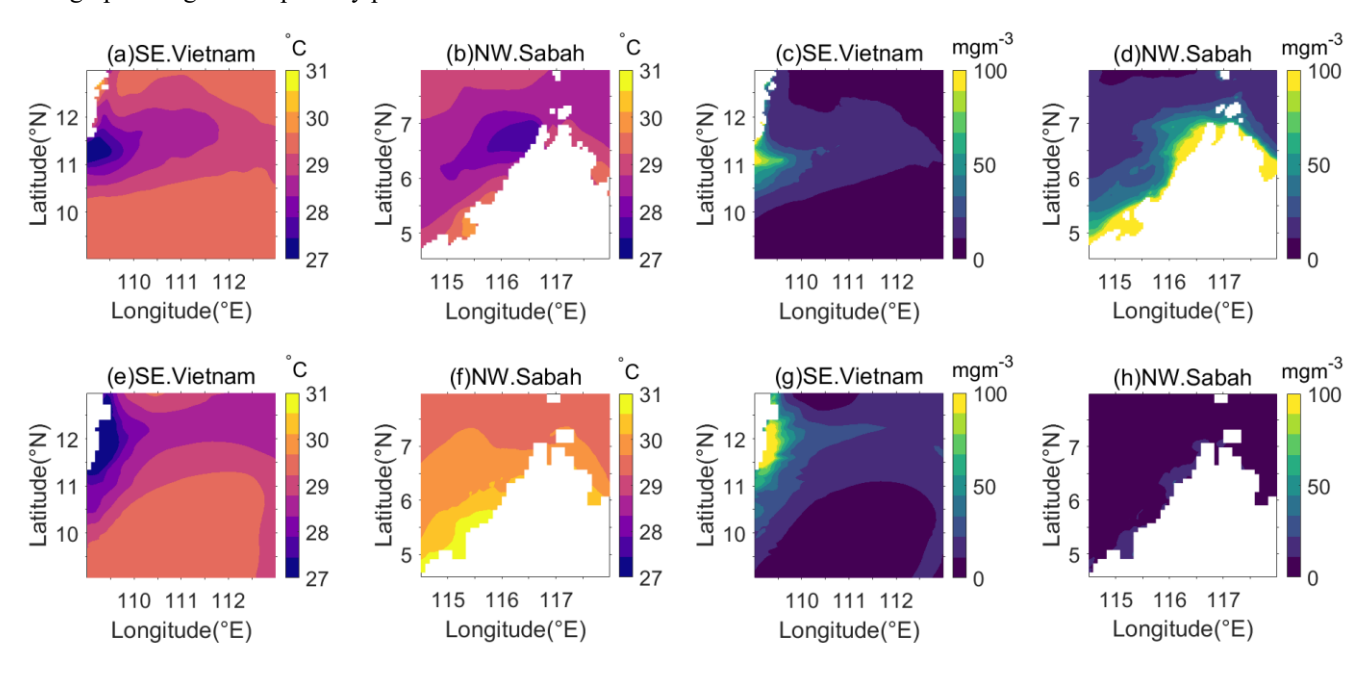


Figure 3: Comparison between observed (a, b) and model-simulated (e, f) mean sea surface temperatures and corresponding mean
Phytoplankton Carbon biomasses (c, d) & (g, h (Converted Chl.-a from satellite data)) in southeast Vietnam and northwest Sabah upwelling regions during their respective upwelling seasons in 2023 (i.e., summer for 2023 and winter for 2023).

## 3.2 Temporal and spatial dynamics of the abiotic environment

# 3.2.1 Temperature

#### 3.2.1.1 Temporal dynamics

The model-predicted mean seawater temperature of the upper 120 m in southeast Vietnam exhibited a significant increasing trend over the 70-year period from 1990 to 2060, with an average increase of 0.02°C per year (R<sup>2</sup> = 0.7573, p < 0.0001: Figure 4.a). Similarly, in northwest Sabah (Figure 4.b), the temperature showed an average increase of 0.03°C per year, which was also statistically significant (R<sup>2</sup> = 0.7899, p < 0.0001: Figure 4.b). Atop these increasing trends, in both upwelling systems, seawater temperature varied notably interannually (Figure 4, b). These model-predicted increasing trends and the





variability around it can also be seen in the anomaly plots (Figure 4.c, d). Here, the calculated seasonal anomalies: (i) became increasingly positive and (ii) more intense towards the end of the simulated timeseries (Figure 4.c, d). However, the magnitudes of the positive anomalies predicted for southeast Vietnam (Figure 4.c) showed a greater variability among the adjacent years when compared to northwest Sabah (Figure 4.d).

# 3.2.1.2 Spatial dynamics

The notable interannual variations of mean seawater temperature of the upper 120 m in both upwelling systems appeared to have at least partly driven by its spatial heterogeneity (Figure 4.e, f). Comparing two decades in the proximal and distal ends of the timeseries, i.e., past (1990-2000) and future (2050-2060), the percentage change in the seasonal means of seawater temperature of the photic zone from 2050 to 2060 was on average 6.62% higher (range = 5.56%-8.05%) compared to the period from 1990 to 2000 in the southeast Vietnam upwelling area (Figure 4.e). In northwest Sabah upwelling area, the corresponding average temperature increase is 6.11% with a range of 5.60% and 6.78% (Figure 4.f). According to the model-predicted spatial distribution pattern of seawater temperature over the upwelling regions, the areas typically characterized by cold upwelled waters have shown more intense temperature changes compared to adjacent open waters (Figure 4.e, f).

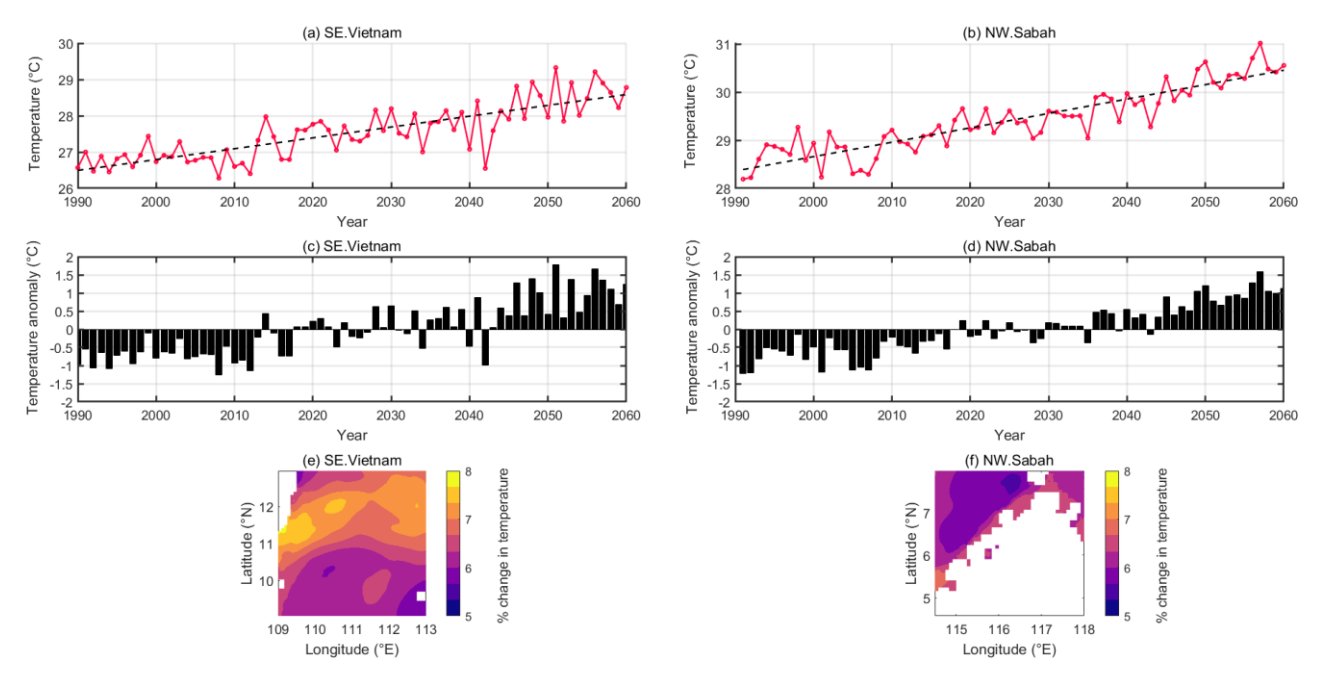


Figure 4: The seasonal mean temperature (a, b) of the upper 120 m of the water column during the upwelling seasons in southeast Vietnam (a) and northwest Sabah (b) predicted by the model for the 1990-2050 timeseries under the IPCC RCP8.5 scenario. Data are presented in °C. The black dotted line represents the trendline fitted to the data. The temperature (c, d) anomaly in southeast Vietnam and northwest Sabah upwelling areas. Percentage change in mean temperature (e, f) of the upper 120 m of the water





column during the upwelling seasons in southeast Vietnam (e) during summer and northwest Sabah (f) during winter from 2050 to 2060 under the RCP8.5 scenario relative to the period 1990-2000.

#### 3.2.2 Nutrients

#### 3.2.2.1 Temporal dynamics

The nitrate concentration in southeast Vietnam exhibited no apparent trend over the simulated 70-year period from 1990 to 2060, with an average decrease of 0.001 mmolN m<sup>-3</sup> per year (R<sup>2</sup> = 0.0039, p = 0.6030: Figure 5.a). Conversely, a statistically significant increasing trend was predicted for Sabha upwelling region, which encountered a 0.003 mmolN m<sup>-3</sup> yr<sup>-1</sup> (R<sup>2</sup> = 0.1403, p = 0.0014: Figure 5.c) mean increase in the nitrate concentration over the simulated timeseries. Despite the observed trends, in both upwelling regions, the model-simulated nitrate concentration shows a considerable interannual variability, which can also be observed in the anomaly plots (Figure 5.e, g).

The silicate concentration showed decreasing trends in both southeast Vietnam (0.015 mmolSi m<sup>-3</sup> yr<sup>-1</sup>) and northwest Sabah upwelling (0.003 mmolSi m<sup>-3</sup> yr<sup>-1</sup>) regions over the simulated 70-year timeseries from 1990 to 2060 (Figure 5.b, d). These observed trends are statistically significant (southeast Vietnam region: R<sup>2</sup> = 0.3162, p < 0.0001, northwest Sabah region: R<sup>2</sup> = 0.2310, p < 0.0001). Moreover, a higher interannual variability is observed in both areas over the period from 1990 to 2060. These model-predicted decreasing trends and the variability around it can also be seen in the anomaly plots (Figure 5.f, h). Here, the calculated seasonal anomalies: (i) became increasingly negative and (ii) more intense towards the end of the simulated timeseries (Figure 5.f, h).

## 3.2.2.2 Spatial dynamics

265

270

275

According to model simulations performed under RCP8.5 scenario, the model-predicted mean nitrate concentration in the southeast Vietnam upwelling area was 2.80 mmolN m<sup>-3</sup> for 1990-2000 period and 2.76 mmolN m<sup>-3</sup> for 2050-2060. As a percentage change, this is an average decline of 0.33% across the two decadal periods (range = -12.77% – 60.22%: Figure 6.a, b). The decline is more pronounced closer to the coast, while the greater range is due to some patches of very high variation (Figure 6.a). In northwest Sabah upwelling area, the average increase of nitrate concentration from 1990-2000 to 2050-2060 periods was 14.45% with a range from 0.30% to 36.62% (Figure 6.b). Here, the nitrate concentration in the upper 120 m increased from 1.91 mmolN m<sup>-3</sup> to 2.09 mmolN m<sup>-3</sup>. However, the increase of mean nitrate concentration closer to the coast is more prominent when compared to the increase observed offshore (Figure 6.b).

The silicate concentration in the southeast Vietnam upwelling area was 3.35 mmolSi m<sup>-3</sup> for 1990-2000 period and 2.48 mmolSi m<sup>-3</sup> for 2050-2060. As a percentage change, this is an average decline of 25.09% across the two decadal periods (range = -46.59% – -10.45%: Figure 6.c). Here, the overall spatial variability is more similar to the pattern observed by the nitrate concentration in the same area. In northwest Sabah upwelling area, the average decline from 1990-2000 to 2050-2060 periods was 9.53% with a range from -44.98% to 25.69% (Figure 6.d). Here, the mean silicate concentration in the upper 120





m decreased from 1.79 mmolSi m<sup>-3</sup> to 1.58 mmolSi m<sup>-3</sup>. The decline observed here is less than that in the southeast Vietnam upwelling area with a comparatively broader range. Furthermore, in northwest Sabah upwelling region, a decline in silicate concentration is observed towards offshore while it shows an increase near the coast (Figure 6.d). This observed spatial variation is similar to the pattern exhibited by nitrate concentration (Figure 6.b)

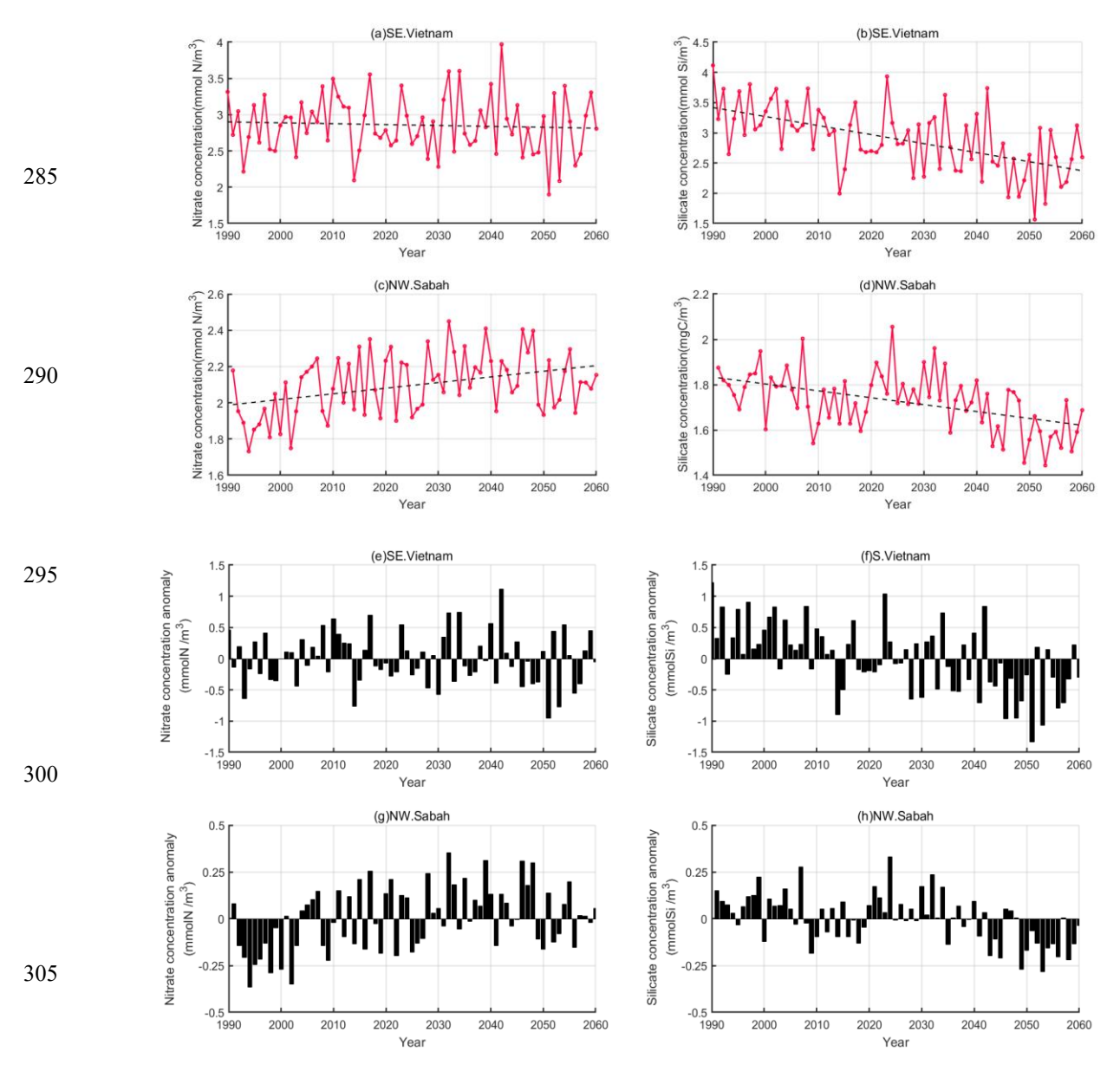
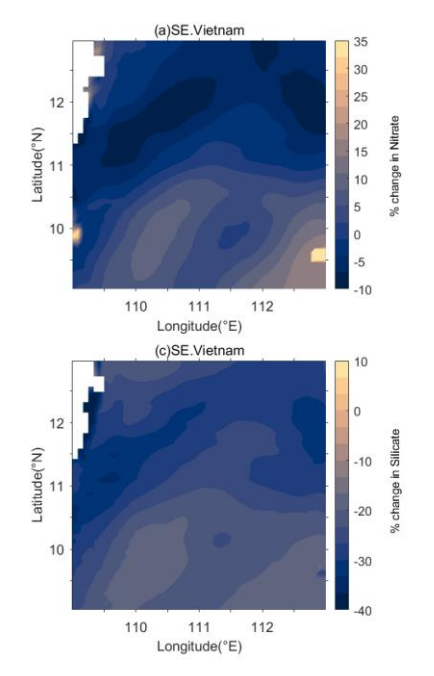


Figure 5: The seasonal mean nitrate (a, c) and silicate (b, d) concentrations of the upper 120 m of the water column during the upwelling seasons in southeast Vietnam (a, b) and northwest Sabah (c, d) predicted by the model for the 1990-2050 timeseries under the IPCC RCP8.5 scenario. Data are presented in mmol m-3. The black dotted line represents the trendline fitted to the data. The nitrate (e, g) and silicate (f, h) concentration anomaly in southeast Vietnam and northwest Sabah upwelling areas.







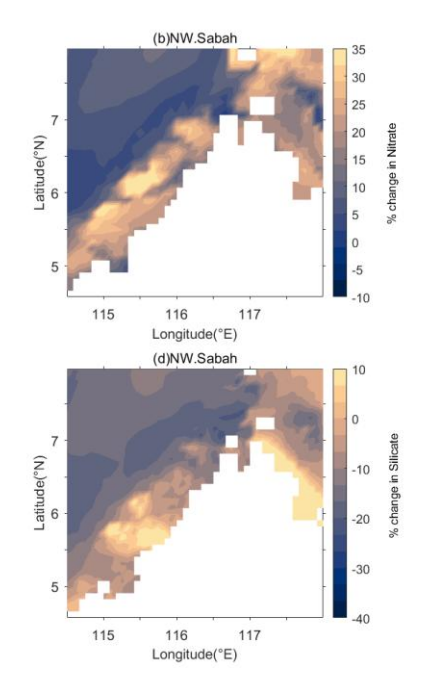


Figure 6: Percentage change in nitrate (a, b) and silicate (c, d) concentrations of the upper 120 m of the water column during the upwelling seasons in southeast Vietnam (a, c) during summer and northwest Sabah (b, d) during winter from 2050 to 2060 under the RCP8.5 scenario relative to the period 1990-2000.

## 3.3 Temporal and spatial dynamics of the biotic environment

## 3.3.1 Temporal and spatial dynamics of the projected phytoplankton biomass

# 315 3.3.1.1 Temporal dynamics

320

The diatom biomass in southeast Vietnam exhibited a significant declining trend over the simulated 70-year period from 1990 to 2060, with an average decrease of 0.027 mgC m<sup>-3</sup> per year (R<sup>2</sup> = 0.0654, p = 0.0314). A similar statistically significant declining trend was predicted for Sabah upwelling region, which encountered a 0.026 mgC m<sup>-3</sup> yr<sup>-1</sup> (R<sup>2</sup> = 0.0813, p = 0.0167) mean decrease in the diatom biomass over the simulated timeseries. Despite these trends, in both upwelling regions, the model-simulated diatom biomass varied considerably year-over-year (Figure 7.a, c). These model-predicted declining trends and the variability around it can also be seen in the anomaly plots (Figure 7.e, g). Here, the calculated seasonal anomalies: (i) became increasingly negative and (ii) more intense towards the end of the simulated timeseries (Figure 7.e, g). However, the magnitudes of the negative anomalies predicted for northwest Sabah (Figure 7.g) were not as pronounced as in southeast Vietnam (Figure 7.e).

The non-diatom biomass also showed a slightly decreasing trend in both southeast Vietnam (0.018 mgC m<sup>-3</sup> yr<sup>-1</sup>) and northwest Sabah upwelling (0.004 mgC m<sup>-3</sup> yr<sup>-1</sup>) regions over the simulated 70-year timeseries from 1990 to 2060 (Figure 7.b, d). However, none of these trends are statistically significant (southeast Vietnam region: R<sup>2</sup> = 0.0304, p = 0.1456, northwest Sabah region: R<sup>2</sup> = 0.0020, p-value: 0.7144). Moreover, according to the calculated seasonal anomalies (Figure

https://doi.org/10.5194/egusphere-2025-4988 Preprint. Discussion started: 17 November 2025





330

335

340

345



7.f, h), a higher interannual variability is observed, while no distinct pattern of increase or decrease in either magnitude or frequency is evident in the upwelling regions of southeast Vietnam and northwest Sabah over the period from 1990 to 2060.

## 3.3.1.2 Spatial dynamics

According to model simulations performed under RCP8.5 scenario, the model-predicted mean diatom biomass in the south Vietnam upwelling area was 11.29 mgC m<sup>-3</sup> for 1990-2000 period and 10.03 mgC m<sup>-3</sup> for 2050-2060. As a percentage change, this is an average decline of 7.09% across the two decadal periods (range = -29.81% – 15.41%:.a). The greater range around this decline signifies the notable spatial variability of diatom biomass (Figure 8.a), where the decline is more pronounced closer to the coast. In contrast, an increase in the diatom biomass of the upper 120 m was predicted by the model in some offshore areas (south and southeastern sectors) of southeast Vietnam upwelling region (Figure 8.a). In northwest Sabah upwelling area, the average decline from1990-2000 to 2050-2060 periods was 11.92% with a range from -30.50% to 30.71% (Figure 8.b). Here, the mean diatom biomass in the upper 120 m decreased from 12.14 mgC m<sup>-3</sup> to 10.63 mgC m<sup>-3</sup>. However, decline of mean diatom biomass closer to the coast is less prominent when compared to the decline observed offshore (Figure 8.b).

The non-diatom biomass in the Southeast Vietnam upwelling area was 15.93 mgC m<sup>-3</sup> for 1990-2000 period and 14.86 mgC m<sup>-3</sup> for 2050-2060. As a percentage change, this is an average decline of 6.15% across the two decadal periods (range = -21.05% – 8.71%:Figure 8.c). Here, the overall spatial variability is more similar to the pattern observed by the diatom biomass in the same area. In northwest Sabah upwelling area, the average decline from1990-2000 to 2050-2060 periods was 0.25% with a range from -16.34% to 12.34% (Figure 8.d). Here, the mean non-diatom biomass in the upper 120 m decreased from 19.26 mgC m<sup>-3</sup> to 18.96 mgC m<sup>-3</sup>. The decline observed here is less than that in the southeast Vietnam upwelling area and also has a comparatively narrower range. Furthermore, in northwest Sabah upwelling region, a decline in non-diatom biomass is observed near the coast while it shows an increase towards offshore. This observed pattern contrasts with the pattern exhibited by diatom biomass (Figure 8.b, d).

355

350

360





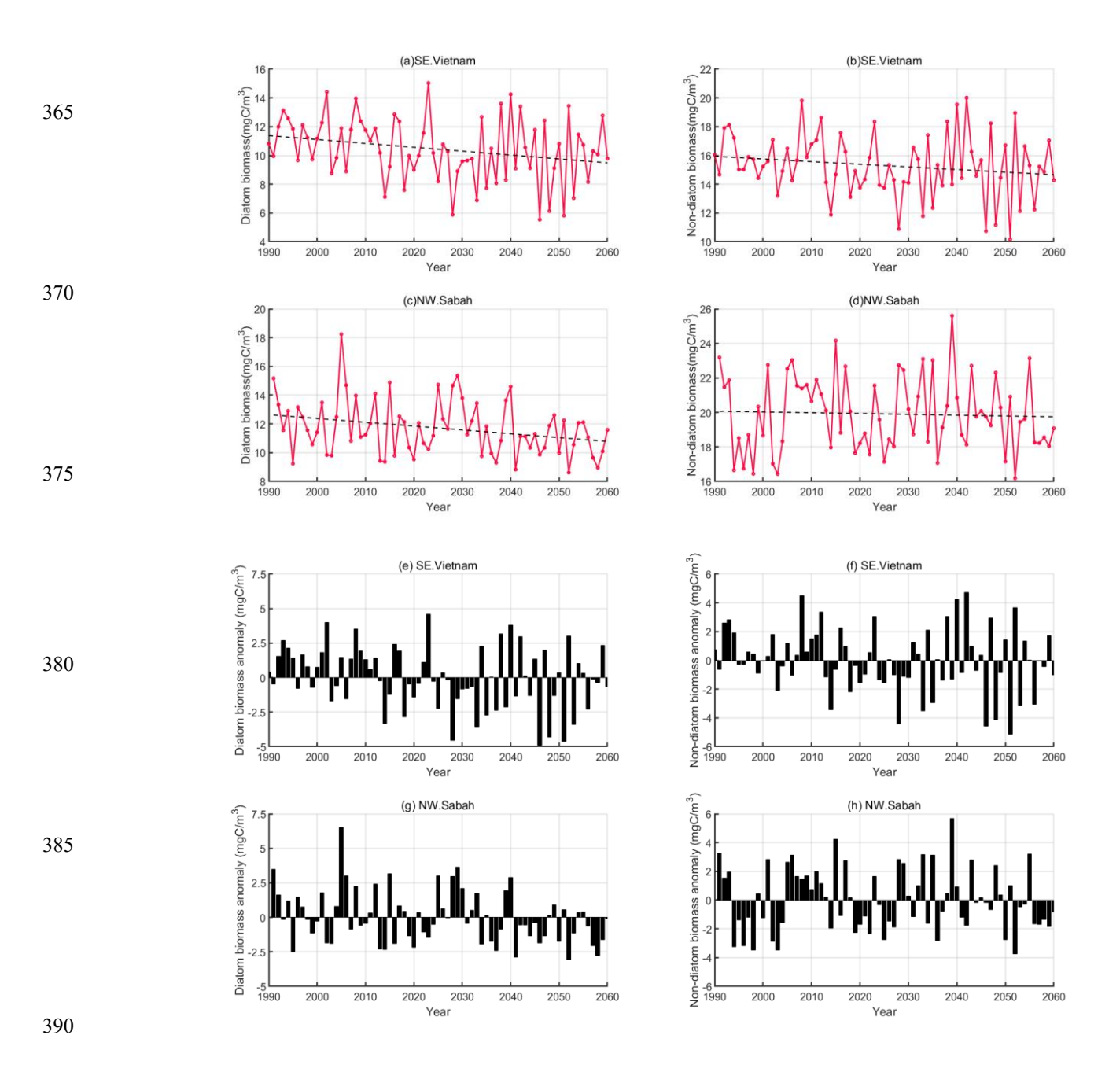
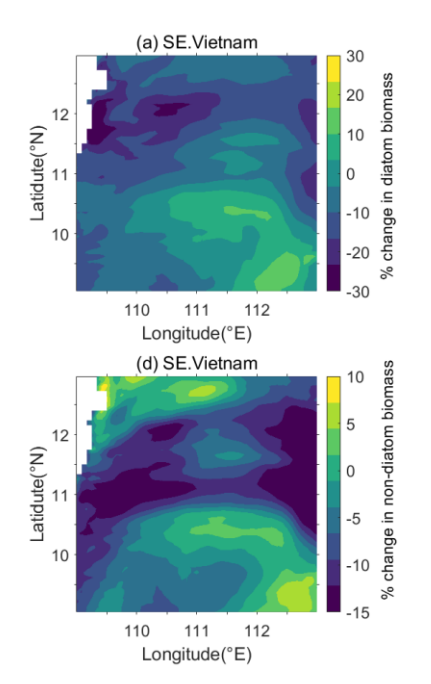


Figure 7: The seasonal mean diatom (a, c) and non-diatom (b, d) biomass of the upper 120 m of the water column during the upwelling seasons in Southeast Vietnam (a, b) and Northwest Sabah (c, d) predicted by the model for the 1990-2050 timeseries under the IPCC RCP8.5 scenario. Data are presented in mgC m-3. The black dotted line represents the trendline fitted to the data. The diatom (e, g) and non-diatom (f, h) biomass anomaly in Southeast Vietnam and Northwest Sabah upwelling areas.







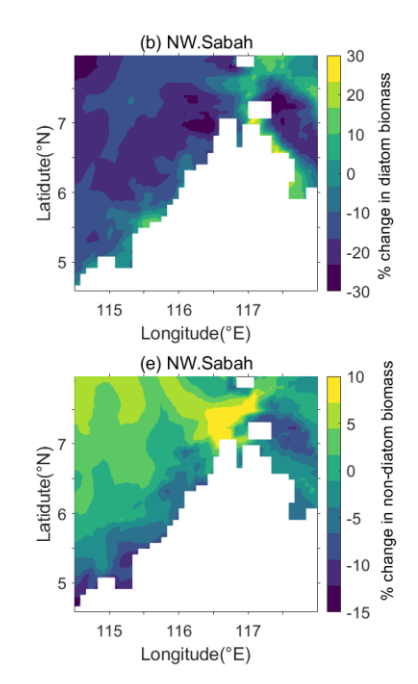


Figure 8: Percentage change in mean diatom (a, b) and non-diatom (c, d) biomass of the upper 120 m of the water column during the upwelling seasons in southeast Vietnam (a, c) during summer and northwest Sabah (b, d) during winter from 2050 to 2060 under the RCP8.5 scenario relative to the period 1990-2000.

# 3.3.2 Temporal and spatial dynamics of the projected grazer biomass

## 3.3.2.1 Temporal dynamics

405

410

The model-predicted mesozooplankton biomass in the upper 120 m of the southeast Vietnam upwelling region exhibited a significant declining trend over the 70-year period (1990-2060), with an average decrease of 0.019 mgC m<sup>-3</sup> per year ( $R^2 = 0.0739$ , p = 0.0219: Figure 9.a). This trend is accompanied by very high interannual variability which is also noticeable in the anomaly plot (Figure 9.c). In northwest Sabah (Figure 9.b), the mesozooplankton biomass showed an average decrease of 0.016 mgC m<sup>-3</sup> per year. However, unlike southeast Vietnam upwelling region, the decreasing trend in Sabah region was not statistically significant ( $R^2 = 0.0364$ , p-value: 0.1137). According to the calculated seasonal anomalies, mesozooplankton biomass become: (i) increasingly negative and (ii) more intense towards the end of the simulated timeseries (Figure 9.c, d).

## 3.3.2.2 Spatial dynamics

Pronounced spatial heterogeneity of grazer distribution in the upper 120 m of the water column was a common characteristic of both upwelling regions (Figure 9.e, f). Consequently, the mean decline of grazer biomass along the timeseries was not





420



spatially homogenous. Instead, according to the model predictions, despite percentage change in the seasonal mean mesozooplankton biomass in the distal decade of the timeseries (2050-2060) decreased by ca. 13.2% compared to the proximal decade (1990-2000), it ranged between -41.59% and 20.71% (Figure 9.e) in the southeast Vietnam upwelling region. The situation in northwest Sabah upwelling area was not different from this where, the average decline of the mesozooplankton biomass in the upper 120 m was 10.65% with a range from -44.98% to 25.69% (Figure 9.f). This massive range is due to the spatial heterogeneity of zooplankton distribution over the two upwelling regions, where the declining trends were some strong increases in some offshore areas in southeast Vietnam (Figure 9.e) and in northern coastal area of Sabah (Figure 9.f). Another observation is that the model-predicted spatial distribution pattern of mesozooplankton biomass in southeast Vietnam region resembled that of both non-diatom and diatom biomasses of the same area (cf. Figure 8.a, c). In contrast, mesozooplankton biomass distribution in northwest Sabah did not exhibit this resemblance.

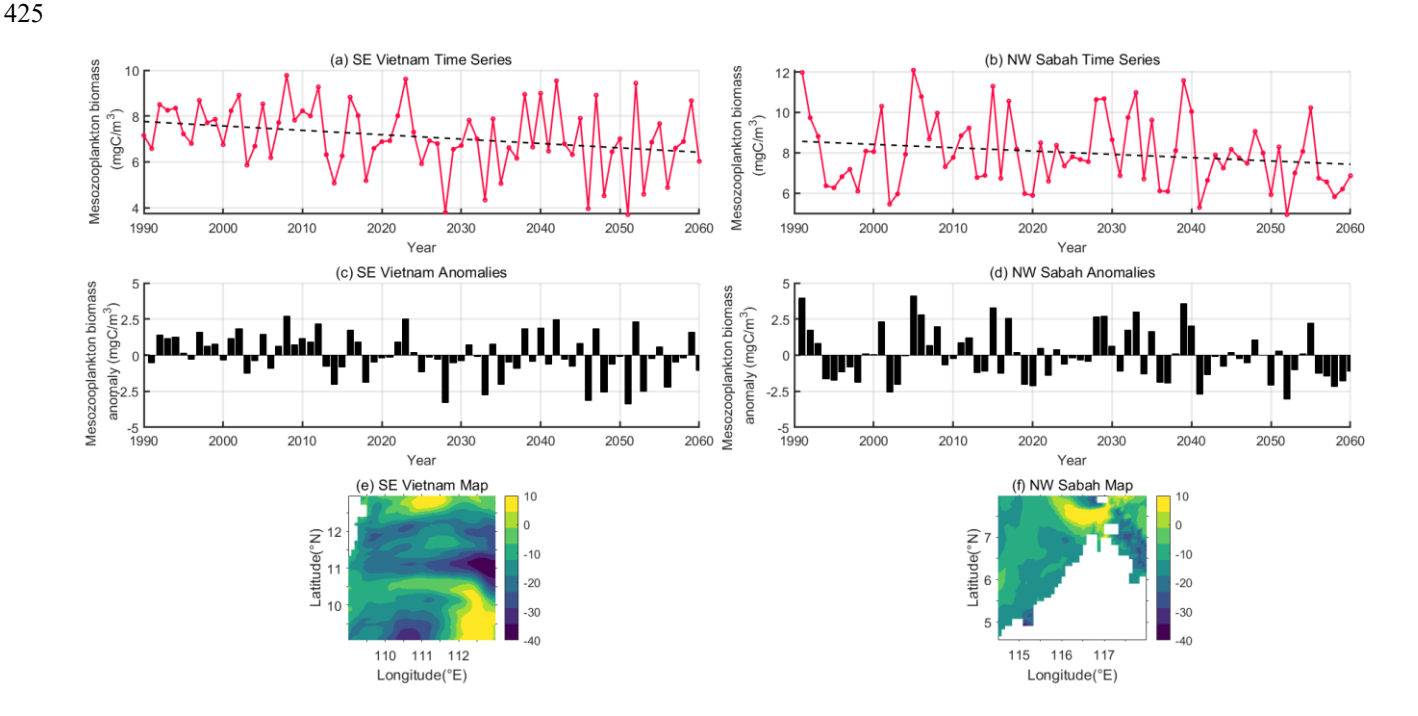


Figure 9: The seasonal mean mesozooplankton biomass (a, b) of the upper 120 m of the water column during the upwelling seasons in southeast Vietnam (a) and northwest Sabah (b) predicted by the model for the 1990-2050 timeseries under the IPCC RCP8.5 scenario. Data are presented in mgC m-3. The black dotted line represents the trendline fitted to the data. The mesozooplankton biomass (c, d) anomaly in southeast Vietnam and northwest Sabah upwelling areas. Percentage change in mean mesozooplankton biomass (e, f) of the upper 120 m of the water column during the upwelling seasons in southeast Vietnam (e) during summer and northwest Sabah (f) during winter from 2050 to 2060 under the RCP8.5 scenario relative to the period 1990-2000.

435

430





## 3.4 Relationships between phytoplankton biomass and selected environmental factors

The general relationships between phytoplankton biomasses (diatom and non-diatom) and the environmental variables that have been discussed in the previous chapters are shown in Figure 10.a, b. The observed relationships between these variables differ across the two regions. In the PCA biplot for southeast Vietnam, PC1 and PC2 collectively explain 88.94% of the total variance in the data, whereas in northwest Sabah, they explain 74.38% of the variance. According to the Pearson's correlation performed, in southeast Vietnam, diatom biomass has shown positive correlations with nitrate (r = 0.64, p< 0.0001), silicate (r = 0.72, p < 0.0001) and mesozooplankton (r = 0.94, p < 0.0001), while a negative correlation is observed with temperature (r = -0.62, p < 0.0001). For non-diatom biomass, positive correlations are observed with nitrate (r = 0.69, p < 0.0001) and mesozooplankton (r = 0.93, p < 0.0001) whereas a negative correlation is observed with temperature (r = -0.61, p < 0.0001).

In northwest Sabah, diatom biomass has shown a positive correlation with mesozooplankton (r = 0.82, p < 0.0001). However, the correlations with nitrate (r = 0.21, p-value: 0.0798) and silicate (r = 0.19, p-value: 0.1037), were positive but not statistically significant. Similar to the findings in southeast Vietnam, diatom biomass in northwest Sabah has shown a negative correlation with temperature (r = -0.39, p-value: 0.0006). For non-diatom biomass, positive correlations are observed with nitrate (r = 0.62, p < 0.0001) and mesozooplankton (r = 0.87, p < 0.0001) whereas a negative correlation is observed with temperature (r = -0.32, p-value: 0.0062).





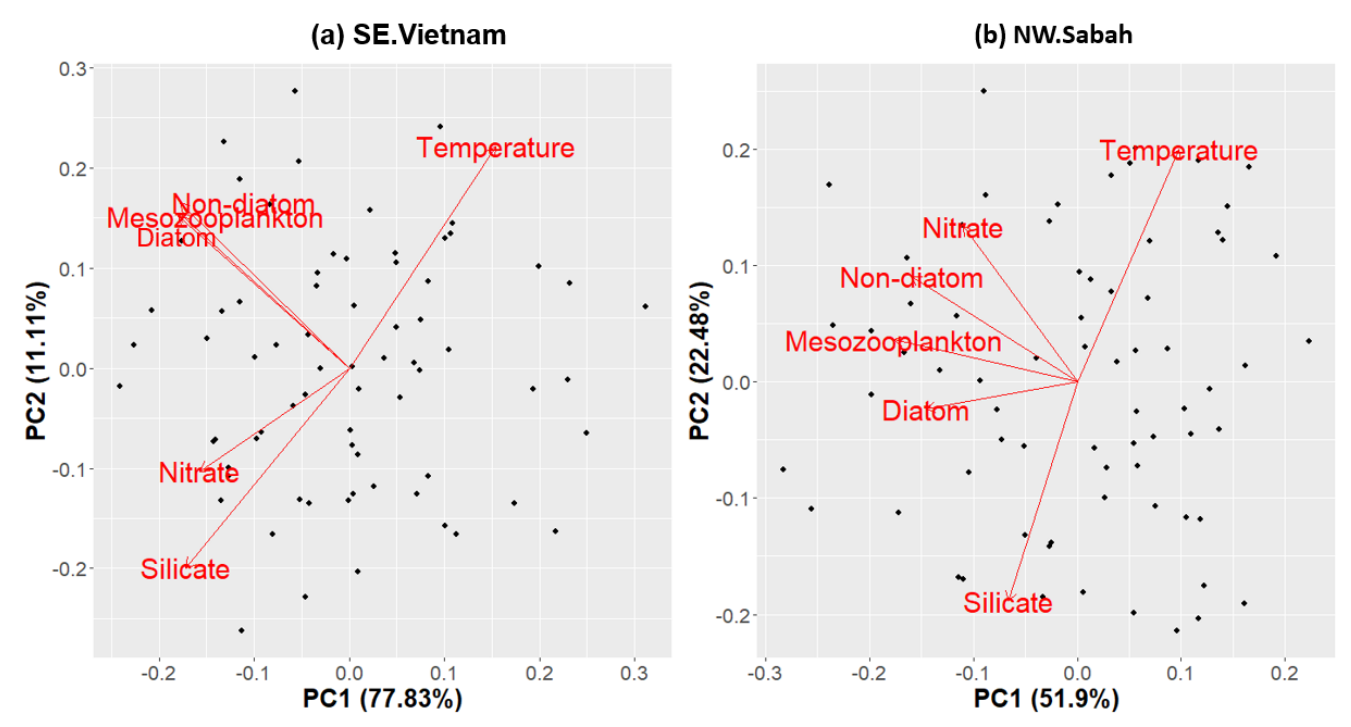


Figure 10: Principal Component Analysis (PCA) of seasonal means of phytoplankton biomass and the selected environmental variables in southeast Vietnam(a) and northwest Sabah(b) Regions (1990-2060). The arrows represent the variables, and the points represent the years. The arrows directed to same direction and are close to each other are positively correlated, arrows in opposite direction are negatively correlated and the arrows that are placed orthogonal have no relationship.

#### 4 Discussion

The present study focused on using output data from a coupled 3D biophysical model to analyze the response of phytoplankton biomass in two selected upwelling regions of the southern South China Sea, to anthropogenic climate change. The results indicate that there is a notable decline in the upper-pelagial (> 120 m) diatom and non-diatom phytoplankton biomass over the analyzed 70-year timeseries (1990-2060: RCP8.5) (Figure 7). These trends are accompanied by rising temperatures, declining silicate concentrations and fluctuating nitrate concentrations within the studied regions (Figure 4,Figure 5). Despite these temporal trends, a significant spatio-temporal heterogeneity was observed in the data, where the model-predicted phytoplankton biomass varied considerably: interannually and spatially across the study area. Statistical analyses revealed inverse relationship between temperature and silicate and a close association between diatom, non-diatom and mesozooplankton biomasses (Figure 10). The declining phytoplankton biomass appeared to have negatively influenced the mesozooplankton grazers in the model, whose biomass also declined over time. This signifies how the impacts of anthropogenic climate change on the tropical ocean's biological productivity can transcend across trophic levels.



475

480

485

490



The decline of pelagic primary producer biomass predicted by the SEAsia model is somewhat consistent with the projections for the tropical western Pacific from previous global-scale studies on primary production (Bopp et al., 2013; Henson et al., 2021; Steinacher et al., 2010). However, since these studies have not specifically focused on the South China Sea, it is interesting to understand the drivers behind the observed decreasing trends in phytoplankton biomass within this region. According to global-scale studies, the projected reduction in primary production in tropics and mid-latitude regions, driven by climate change, is primarily caused by enhanced stratification, which results in decreased nutrient availability due to poor vertical mixing (Bopp et al., 2013; Chust et al., 2014; Dutkiewicz et al., 2013; Marinov et al., 2010).

The present study predicts rising temperatures, potentially intensifying stratification along the studied period until 2060 (Figure 4. a, b). This stratification is likely causing the declining nutrient concentration trends, as evidenced by the declining silicate concentrations observed in this study (Figure 5. b, d). However, nitrate concentrations observed in both study areas did not follow this trend (Figure 5. a, c). These contrasting patterns could be due to differing regional oceanographic features. In the southeastern Vietnam upwelling area, specifically the nitrate dynamics are influenced not only by upwelling but also by Mekong River runoff (Bombar et al., 2010). Similarly, in the northwestern Sabah upwelling area, nutrient dynamics are affected by both upwelling and coastal river discharge (Baram river and Padas river), as well as surface water transport (Abbas et al., 2012), which may have contributed to these changes. Moreover, the decline in silicate driven by warming-induced stratification may have impacted the observed reduction in diatom biomass. However, the observed silicate decline had little impact on non-diatom biomass, as observed by their declines, which were not statistically significant. In addition to the dependency on the discussed factors, biomass in the model relies on photosynthetically active radiation (PAR) (Butenschön et al., 2016). However, this is not analysed in the present study, as solar radiation is abundant in tropical regions, making nutrients a comparatively more significant limiting factor (Zhao et al., 2018).



500

505

510



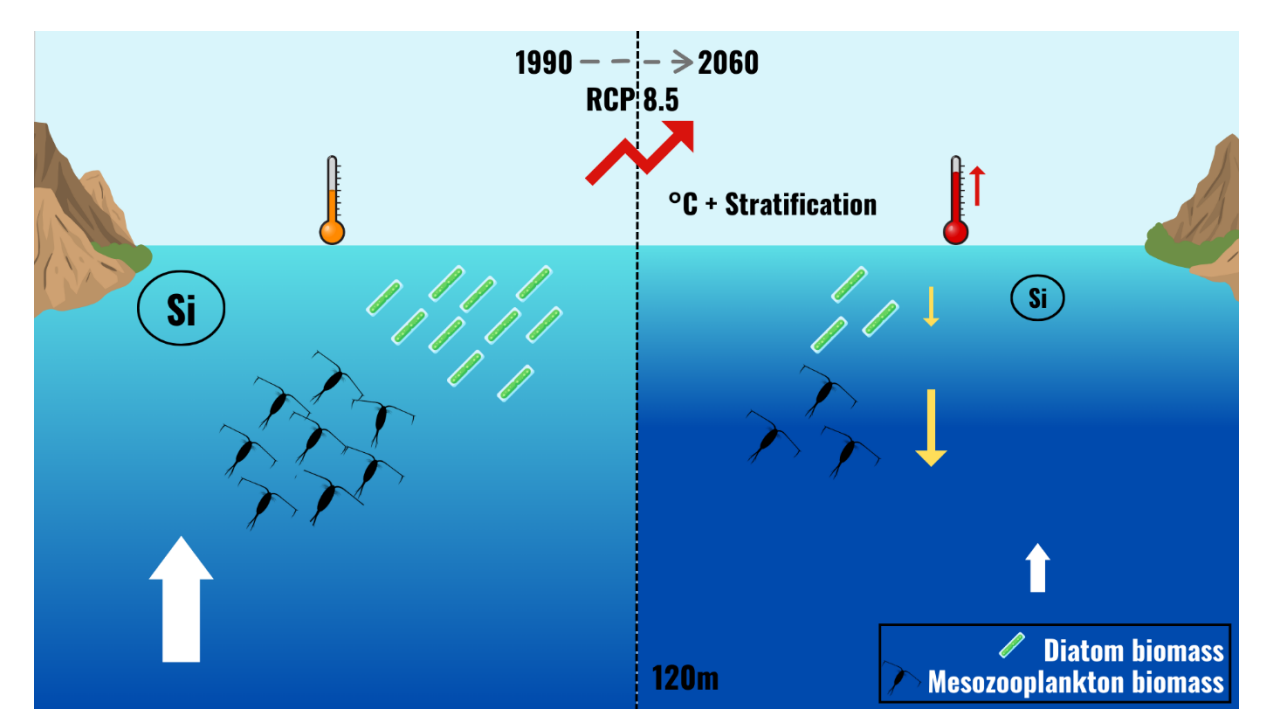


Figure 11: Schematic diagram summarizing the key results, illustrating an increasing trend in temperature according to the IPCC RCP8.5 climate scenario, likely increasing stratification of water column projected from 1990 to 2060. The diagram indicates how enhanced stratification has reduced upwelled nutrients (particularly silicate as observed in this study), resulting in a reduction in diatom biomass. This reduction is reflected in mesozooplankton biomass but in a greater magnitude, highlighting the transfer of climate change impacts across trophic levels. The width of the arrows in the diagram represents the magnitude of these changes, with upward arrows indicating increasing trends and downward arrows indicating decreasing trends.

These results show that temperature and silicate imposed notable bottom-up control over the model-predicted phytoplankton biomass. Previous studies (e.g., Winder & Sommer, 2012) indicate that temperature significantly affects heterotrophic metabolism when compared to primary production. Warming is thus expected to boost grazing pressure, which imposes a stronger top-down control on phytoplankton. However, according to the present study, both phytoplankton (diatom and non-diatom) and grazer (mesozooplankton) biomasses have declined over the simulated timeseries (Figure 7, Figure 9.a, b). For example, in southeastern Vietnam upwelling region, the reduction of the diatom biomass from 1990 to 2060 was 7.09% while mesozooplankton exhibited a biomass reduction of 13.20%, which is nearly two-fold compared to phytoplankton. This indicates that rising temperatures, limited nutrients (silicate) and declining phytoplankton biomass had a negative impact on the mesozooplankton biomass (Figure 10). This resembles the findings of Lewandowska et al., (2014) that in thermally-stratified, nutrient-limited waters, mesozooplankton (copepods) switch from feeding primarily on phytoplankton (diatoms) to smaller protists, such as ciliates – thus signifying the relative importance of the microbial loop. However, since diatoms have a much higher nutritional value compared to protists, this change may result in an overall decline in the mesozooplankton biomass. Despite the declining mesozooplankton biomass relaxed the grazing pressure on phytoplankton, the phytoplankton biomass simulated in the SEAsia model did not increase consequently (Figure 7, Figure 9.a, b). This indicates that bottom-up forcing – i.e., temperature and nutrients had a much greater influence on the phytoplankton biomass than the grazing



515

520

525

530

535

540

545



pressure on the top-down. Figure 11 summarizes these key results discussed above. However, some caution is necessary when interpreting these results, as biases may emerge from spatially averaging each variable across the selected domains. Nevertheless, a significant interannual variability remains even after spatial averaging, highlighting the inherent fluctuations within each region.

In this study, the grazing pressure was characterized by the zooplankton biomass in the upper pelagial. There are two limitations of this approach. Firstly, the present analyses do not consider the vertical overlap between phyto- and zooplankton but focus on depth-averaged estimates for simplicity. Vertical positioning of predator and prey is an important metric that needs to be characterized in the future when further analyzing this dataset to render more accurate understanding of the grazing pressure (Cáceres et al., 2013; Greer et al., 2013). This is of particular significance given that both zooplankton and motile phytoplankton can perform tens-to-hundreds of meters deep diel vertical migrations (Brierley, 2014), which is not a part of SEAsia simulations. Secondly, this model accounts for neither plasticity nor evolution of body size among plankton. Recent individual based models have shown that especially, mesozooplankton body size is highly plastic to environmental variables, such as seawater temperature and phytoplankton concentration (Evans et al., 2020; Maps et al., 2012). Body size is a master life-history trait that can alter grazing, growth, developmental, metabolic and reproductive rates through allometric relationships (Carey & Sigwart, 2014). Further, models have shown that climate change driven shifts in thermal and feeding regimes in the ocean can lead to decrease in the average body size of mesozooplankton grazers (herbivorous copepods) and make them more numerous (Hays et al., 2005; Richardson, 2008). However, the SEAsia model does not consider the manifestations of zooplankton body size plasticity/evolution on phytoplankton biomass dynamics. Therefore, the present analyses may not render a full picture of the top-down selection pressure on phytoplankton dynamics. Despite the limitations of the characterization of selection pressures, some key environmental variables aligned well with field observations. For example, the model-predicted temperature showed a good agreement with the satellite-observed temperature (Figure 3.a, b), despite adopting forcing based on IPCC RCP8.5scenario, which may account for the observed changes in the comparison (Figure 3.e, f). In addition, the observed pattern of cold-water masses in southeast Vietnam in the model aligned well with the movement of eastward surface jets observed in this region during the summer monsoon season (Hermann et al., 2013). Similarly, the general near-surface spatial distribution pattern of phytoplankton biomass (carbon) was corroborated by satellite observations (Figure 3.c, d). However, the numerical phytoplankton biomass estimates did not match well with the observations (Figure 3.g, h), possibly due to satellite-derived product being Chl.-a – an entity that was missing from the ERSEM configuration coupled to the SEAsia model.

An overarching prediction of the present study is the negative (bottom-up) impact of the declining phytoplankton biomass on the adjacent trophic level (mesozooplankton grazers) in the studied upwelling areas of the southern South China Sea. It is understood that temperature-driven climate change impacts can intensify along marine food chains, because higher trophic levels are more sensitive to thermal stress and food depletion (Hu et al., 2022). In this specific case, it is worthy of investigating how far up the trophic chain that the impact of food depletion (= decrease of phyto- and mesozooplankton biomass) would reverberate within these two highly productive upwelling regions of the SSCS. In the SSCS, higher up in the



550

555



food chain are various mesopelagic and epipelagic fish that for at least some part of their life cycle feed on zooplankton (e.g., herring, anchovies, younger stages of mackerel). These fish are commercially harvested and fish landings of the south China Sea accounts for staggering 12% of the world's capture fisheries (11-17 million tonnes by 2000s: Pauly & Liang, 2020; Teh et al., 2017). However, fish catches of this region have been declining lately due to overfishing and habitat destruction (Pitcher et al., 2000). Unfortunately, the current fisheries projections and management efforts in the (S)SCS do not consider the potential climate change impacts unraveled by the present study. Recent examples from some North Sea fish stocks (Dickey-Collas et al., 2010) show that when climate change impacts interact with other anthropogenic factors (e.g., overfishing) it can cumulate into catastrophic ecological and socioeconomic consequences. The SSCS pelagic ecosystem is already in an alarming state and how climate change driven decline of planktonic biomass would amplify this crisis should thus be investigated in detail before it is too late. The present study is, therefore, a small yet significant step in the correct direction, that needs to be expanded in the future.

#### **5 Conclusion**

This study provides insights on the potential effects of anthropogenic climate change on phytoplankton biomass, particularly diatom, in the southern South China Sea by mid-century. Model predictions based on the SEAsia coupled 3D biophysical model outputs under the RCP 8.5 climate scenario have shown that the phytoplankton biomass (diatom and non-diatom) will decline from 1990 to 2060. This decline is accompanied by rising temperature trends likely leading to reduced nutrient concentrations, particularly silicate, possibly due to the warming-induced stratification that reduces upwelling. In addition to the declining phytoplankton biomass trends, the model predictions also indicate a declining trend in grazer biomass (mesozooplankton). Despite this release of the predation pressure on phytoplankton, which could have favoured an increase in the phytoplankton biomass, the decline has persisted, highlighting the influence of the bottom-up control within this ecosystem. Furthermore, the decline in mesozooplankton biomass is nearly two-fold in comparison to diatom biomass decline, which underlines the amplification of climate change induced impacts across trophic levels. To conclude this work, we recommend further research on the phytoplankton dynamics in relation to climate change in this region to better understand of its impacts and to determine to which extent these climate change impacts cascade across the trophic levels.

#### 6 Author contribution

575

The work, methodologies, and formal analysis were conceptualized by CK. The article was authored by CK, with input from all co-authors. Work supervision was conducted by MFA, NG, KB, RA. All authors contributed to the article and endorsed the submitted version.





#### References

- Abbas, A., Mansor, S., Pradhan, B., & Tan, C. K. (2012). *Spatial and seasonal variability of Chlorophyll-a and associated oceanographic events in Sabah water*. 215–219. https://doi.org/10.1109/EORSA.2012.6261168
  - Abdul-Hadi, A., Mansor, S., Pradhan, B., & Tan, C. K. (2012). Seasonal variability of chlorophyll-a and oceanographic conditions in Sabah waters in relation to Asian monsoon—A remote sensing study. *Environmental Monitoring and Assessment*, 185. https://doi.org/10.1007/s10661-012-2843-2
- Akhir, M. F. (2012). Surface Circulation and Temperature Distribution of Southern South China Sea from Global Ocean Model (OCCAM). *Sains Malaysiana*, *41*, 701–714.
  - Akhir, M. F., Daryabor, F., Husain, M., Tangang, F., & Qiao, F.-L. (2015). Evidence of Upwelling along Peninsular Malaysia during Southwest Monsoon. *Open Journal of Marine Science*, *5*, 273–279. https://doi.org/10.4236/ojms.2015.53022
- Apriansyah, A., Atmadipoera, A., Jaya, I., Nugroho, D., & Akhir, M. F. (2022). Seasonal oceanographic changes and their implications for the abundance of small pelagic fishes in the southern South China Sea. *Regional Studies in Marine Science*, 54, 102499. https://doi.org/10.1016/j.rsma.2022.102499
  - Behrenfeld, M. J., O'Malley, R. T., Siegel, D. A., McClain, C. R., Sarmiento, J. L., Feldman, G. C., Milligan, A. J., Falkowski, P. G., Letelier, R. M., & Boss, E. S. (2006). Climate-driven trends in contemporary ocean productivity. *Nature*, 444(7120), 752–755. https://doi.org/10.1038/nature05317
- 595 Bindoff, N. L., Cheung, W. W. L., Kairo, J. G., Arístegui, J., Guinder, V. A., Hallberg, R., Hilmi, N., Jiao, N., O'Donoghue, S., Suga, T., Acar, S., Alava, J. J., Allison, E., Arbic, B., Bambridge, T., Boyd, P. W., Bruggeman, J., Butenschön, M., Chávez, F. P., ... Whalen, C. (2019). Changing Ocean, Marine Ecosystems, and Dependent Communities. *Marine Ecosystems*.
- Bombar, D., Dippner, J. W., Doan, H. N., Ngoc, L. N., Liskow, I., Loick-Wilde, N., & Voss, M. (2010). Sources of new nitrogen in the Vietnamese upwelling region of the South China Sea. *Journal of Geophysical Research: Oceans*, 115(C6). https://doi.org/10.1029/2008JC005154
  - Bopp, L., Resplandy, L., Orr, J. C., Doney, S. C., Dunne, J. P., Gehlen, M., Halloran, P., Heinze, C., Ilyina, T., Séférian, R., Tjiputra, J., & Vichi, M. (2013). Multiple stressors of ocean ecosystems in the 21st century: Projections with CMIP5 models. *Biogeosciences*, 10(10), 6225–6245. https://doi.org/10.5194/bg-10-6225-2013
- Boyce, D. G., Lewis, M. R., & Worm, B. (2010). Global phytoplankton decline over the past century. *Nature*, 466(7306), 591–596. https://doi.org/10.1038/nature09268
  - Brierley, A. S. (2014). Diel vertical migration. *Current Biology*, 24(22), R1074–R1076. https://doi.org/10.1016/j.cub.2014.08.054
  - DRAKKAR Group, 2007: Eddy permitting ocean circulation hindcasts of past decades. CLIVAR Exchanges, 42, 8–10.
- 610 Butenschön, M., Clark, J., Aldridge, J. N., Allen, J. I., Artioli, Y., Blackford, J., Bruggeman, J., Cazenave, P., Ciavatta, S., Kay, S., Lessin, G., van Leeuwen, S., van der Molen, J., de Mora, L., Polimene, L., Sailley, S., Stephens, N., & Torres, R. (2016). ERSEM 15.06: A generic model for marine biogeochemistry and the ecosystem dynamics of the lower trophic levels. *Geoscientific Model Development*, 9(4), 1293–1339. https://doi.org/10.5194/gmd-9-1293-2016





- Cáceres, C., Taboada, F. G., Höfer, J., & Anadón, R. (2013). Phytoplankton Growth and Microzooplankton Grazing in the Subtropical Northeast Atlantic. *PLoS ONE*, *8*(7), e69159. https://doi.org/10.1371/journal.pone.0069159
  - Cao, L., Eby, M., Ridgwell, A., Caldeira, K., Archer, D., Ishida, A., Joos, F., Matsumoto, K., Mikolajewicz, U., Mouchet, A., Orr, J. C., Plattner, G.-K., Schlitzer, R., Tokos, K., Totterdell, I., Tschumi, T., Yamanaka, Y., & Yool, A. (2009). The role of ocean transport in the uptake of anthropogenic CO<sub>2</sub>. *Biogeosciences*, *6*(3), 375–390. https://doi.org/10.5194/bg-6-375-2009
- Carey, N., & Sigwart, J. D. (2014). Size matters: Plasticity in metabolic scaling shows body-size may modulate responses to climate change. *Biology Letters*, *10*(8), 20140408. https://doi.org/10.1098/rsbl.2014.0408
  - Chen, Y., Shi, H., & Zhao, H. (2021). Summer Phytoplankton Blooms Induced by Upwelling in the Western South China Sea. *Frontiers in Marine Science*, *8*, 740130. https://doi.org/10.3389/fmars.2021.740130
  - Chust, G., Allen, J. I., Bopp, L., Schrum, C., Holt, J., Tsiaras, K., Zavatarelli, M., Chifflet, M., Cannaby, H., Dadou, I., Daewel, U., Wakelin, S. L., Machu, E., Pushpadas, D., Butenschon, M., Artioli, Y., Petihakis, G., Smith, C., Garçon, V., ...
- Irigoien, X. (2014). Biomass changes and trophic amplification of plankton in a warmer ocean. *Global Change Biology*, 20(7), 2124–2139. https://doi.org/10.1111/gcb.12562
  - Dickey-Collas, M., Nash, R., Brunel, T., van Damme, C., Marshall, C., Payne, M., Corten, A., Geffen, A., Peck, M., Hatfield, E., Hintzen, N., Enberg, K., Kell, L., & Simmonds, J. (2010). Lessons learned from stock collapse and recovery of North Sea herring: A review. *ICES Journal of Marine Science*, 67, 1875–1886. https://doi.org/10.1093/icesjms/fsq033
- Dutkiewicz, S., Scott, J. R., & Follows, M. J. (2013). Winners and losers: Ecological and biogeochemical changes in a warming ocean. *Global Biogeochemical Cycles*, 27(2), 463–477. https://doi.org/10.1002/gbc.20042
  - Evans, L. E., Hirst, A. G., Kratina, P., & Beaugrand, G. (2020). Temperature-mediated changes in zooplankton body size: Large scale temporal and spatial analysis. *Ecography*, 43(4), 581–590. https://doi.org/10.1111/ecog.04631
- Field, C. B., Behrenfeld, M. J., Randerson, J. T., & Falkowski, P. (1998). Primary Production of the Biosphere: Integrating Terrestrial and Oceanic Components. *Science*, 281(5374), 237–240. https://doi.org/10.1126/science.281.5374.237
  - Greer, A. T., Cowen, R. K., Guigand, C. M., McManus, M. A., Sevadjian, J. C., & Timmerman, A. H. V. (2013). Relationships between phytoplankton thin layers and the fine-scale vertical distributions of two trophic levels of zooplankton. *Journal of Plankton Research*, 35(5), 939–956. https://doi.org/10.1093/plankt/fbt056
- Hays, G., Richardson, A., & Robinson, C. (2005). Climate change and marine plankton. *Trends in Ecology & Evolution*, 20, 337–344. https://doi.org/10.1016/j.tree.2005.03.004
  - Henson, S. A., Cael, B. B., Allen, S. R., & Dutkiewicz, S. (2021). Future phytoplankton diversity in a changing climate. *Nature Communications*, *12*(1), 5372. https://doi.org/10.1038/s41467-021-25699-w
  - Hermann, A. J., Gibson, G. A., Bond, N. A., Curchitser, E. N., Hedstrom, K., Cheng, W., Wang, M., Stabeno, P. J., Eisner, L., & Cieciel, K. D. (2013). A multivariate analysis of observed and modeled biophysical variability on the Bering Sea shelf:
- Multidecadal hindcasts (1970–2009) and forecasts (2010–2040). *Deep Sea Research Part II: Topical Studies in Oceanography*, 94, 121–139. https://doi.org/10.1016/j.dsr2.2013.04.007
  - Hou, L.-T., Wang, B.-S., Lai, C.-C., Chen, T.-Y., Shih, Y.-Y., Shiah, F.-K., & Ko, C.-Y. (2022). Effects of Mixed Layer Depth on Phytoplankton Biomass in a Tropical Marginal Ocean: A Multiple Timescale Analysis. *Earth's Future*, *10*(5), e2020EF001842. https://doi.org/10.1029/2020EF001842
- Hu, J., & Wang, X. H. (2016). Progress on upwelling studies in the China seas. *Reviews of Geophysics*, *54*(3), 653–673. https://doi.org/10.1002/2015RG000505





- Hu, N., Bourdeau, P. E., Harlos, C., Liu, Y., & Hollander, J. (2022). Meta-analysis reveals variance in tolerance to climate change across marine trophic levels. *Science of The Total Environment*, 827, 154244. https://doi.org/10.1016/j.scitotenv.2022.154244
- 655 IPCC, 2014: Climate Change 2014: Synthesis Report. Contribution of Working Groups I, II and III to the Fifth Assessment Report of the Intergovernmental Panel on Climate Change [Core Writing Team, R.K. Pachauri and L.A. Meyer (eds.)]. IPCC, Geneva, Switzerland, 151 pp.

  Lewandowska, A. M., Boyce, D. G., Hofmann, M., Matthiessen, B., Sommer, U., & Worm, B. (2014). Effects of sea surface warming on marine plankton. *Ecology Letters*, 17(5), 614–623. https://doi.org/10.1111/ele.12265
- 660 Lindsey, R. (2024, April 9). *Climate Change: Atmospheric Carbon Dioxide* | *NOAA Climate.gov*. http://www.climate.gov/news-features/understanding-climate/climate-change-atmospheric-carbon-dioxide
  - Liu, K.-K., Chao, S.-Y., Shaw, P.-T., Gong, G.-C., Chen, C.-C., & Tang, T. Y. (2002). Monsoon-forced chlorophyll distribution and primary production in the South China Sea: Observations and a numerical study. *Deep Sea Research Part I: Oceanographic Research Papers*, 49(8), 1387–1412. https://doi.org/10.1016/S0967-0637(02)00035-3
- Maps, F., Pershing, A. J., & Record, N. R. (2012). A generalized approach for simulating growth and development in diverse marine copepod species. *ICES Journal of Marine Science*, 69(3), 370–379. https://doi.org/10.1093/icesjms/fsr182
  - Marinov, I., Doney, S. C., & Lima, I. D. (2010). Response of ocean phytoplankton community structure to climate change over the 21st century: Partitioning the effects of nutrients, temperature and light. *Biogeosciences*, 7(12), 3941–3959. https://doi.org/10.5194/bg-7-3941-2010
- Naselli-Flores, L., & Padisák, J. (2023). Ecosystem services provided by marine and freshwater phytoplankton. *Hydrobiologia*, 850(12), 2691–2706. https://doi.org/10.1007/s10750-022-04795-y
  - Pagès, R., Baklouti, M., Barrier, N., Ayache, M., Sevault, F., Somot, S., & Moutin, T. (2020). Projected Effects of Climate-Induced Changes in Hydrodynamics on the Biogeochemistry of the Mediterranean Sea Under the RCP 8.5 Regional Climate Scenario. *Frontiers in Marine Science*, 7. https://doi.org/10.3389/fmars.2020.563615
- Pauly, D., & Liang, C. (2020). The fisheries of the South China Sea: Major trends since 1950. *Marine Policy*, 121, 103584. https://doi.org/10.1016/j.marpol.2019.103584
  - Pierce D (2023). \_ncdf4: Interface to Unidata netCDF (Version 4 or Earlier) Format Data Files\_. R package version 1.22, https://CRAN.R-project.org/package=ncdf4
- Pitcher, T., Watson, R., Haggan, N., Guenette, S., Kennish, R., Sumaila, R., Cook, D., Wilson, K., & Leung, A. (2000).
   Marine Reserves and the Restoration of Fisheries and Marine Ecosystems in the South China Sea. *Bulletin of Marine Science*, 66, 543–566.
  - Richardson, A. J. (2008). In hot water: Zooplankton and climate change. *ICES Journal of Marine Science*, 65(3), 279–295. https://doi.org/10.1093/icesjms/fsn028
- RStudio Team. (2023). RStudio: Integrated Development Environment for R (Version 2023.12.1 402) [Computer software]. RStudio, PBC. http://www.rstudio.com/
  - Satar, M. N., Mohd Fadzil Akhir, Poh Heng Kok, & Daud, N. R. (2020). *Upwelling in the northwest Sabah during the northeast monsoon and its relation with El-Niño*. Unpublished. https://doi.org/10.13140/RG.2.2.29929.11364





- Steinacher, M., Joos, F., Frölicher, T. L., Bopp, L., Cadule, P., Cocco, V., Doney, S. C., Gehlen, M., Lindsay, K., Moore, J. K., Schneider, B., & Segschneider, J. (2010). Projected 21st century decrease in marine productivity: A multi-model analysis. 690 *Biogeosciences*, 7(3), 979–1005. https://doi.org/10.5194/bg-7-979-2010
  - Teh, L. S. L., Witter, A., Cheung, W. W. L., Sumaila, U. R., & Yin, X. (2017). What is at stake? Status and threats to South China Sea marine fisheries. *Ambio*, 46(1), 57–72. https://doi.org/10.1007/s13280-016-0819-0
  - The MathWorks Inc. (2023). MATLAB version: 23.2.0.2485118 (R2023b), Natick, Massachusetts: The MathWorks Inc. <a href="https://www.mathworks.com">https://www.mathworks.com</a>
- 695 Wickham, H. ggplot2: Elegant Graphics for Data Analysis. Springer-Verlag New York, 2016.
  - Winder, M., & Sommer, U. (2012). Phytoplankton response to a changing climate. *Hydrobiologia*, 698(1), 5–16. https://doi.org/10.1007/s10750-012-1149-2
- Wu, C.-R., Wang, L.-C., Wang, Y.-L., Lin, Y.-F., Chiang, T.-L., & Hsin, Y.-C. (2019). Coherent Response of Vietnam and Sumatra-Java Upwellings to Cross-Equatorial Winds. *Scientific Reports*, 9(1), 3650. https://doi.org/10.1038/s41598-019-700 40246-w
  - Xiao, F., Wu, Z., Lyu, Y., & Zhang, Y. (2020). Abnormal Strong Upwelling off the Coast of Southeast Vietnam in the Late Summer of 2016: A Comparison with the Case in 1998. *Atmosphere*, 11(9), 940. https://doi.org/10.3390/atmos11090940
- Xu, W., Wang, G., Jiang, L., Cheng, X., Zhou, W., & Cao, W. (2021). Spatiotemporal Variability of Surface Phytoplankton Carbon and Carbon-to-Chlorophyll a Ratio in the South China Sea Based on Satellite Data. *Remote Sensing*, *13*(1), Article 1. https://doi.org/10.3390/rs13010030
  - Yuan, Z., Liu, D., Keesing, J. K., Zhao, M., Guo, S., Peng, Y., & Zhang, H. (2018). Paleoecological evidence for decadal increase in phytoplankton biomass off northwestern Australia in response to climate change. *Ecology and Evolution*, 8(4), 2097–2107. https://doi.org/10.1002/ece3.3836
- Zhao, H., Zhao, J., Sun, X., Chen, F., & Han, G. (2018). A strong summer phytoplankton bloom southeast of Vietnam in 2007, a transitional year from El Niño to La Niña. *PLoS ONE*, *13*(1), e0189926. https://doi.org/10.1371/journal.pone.0189926
  - Zhu, Y., Liu, J., Mulholland, M. R., Du, C., Wang, L., Widner, B., Huang, T., Yang, Y., & Dai, M. (2021). Dynamics of ammonium biogeochemistry in an oligotrophic regime in the South China Sea. *Marine Chemistry*, 237, 104040. https://doi.org/10.1016/j.marchem.2021.104040

715